ELSEVIER

Computational Materials Science 9 (1997) 229–236

COMPUTATIONAL MATERIALS SCIENCE

Recent advances in modelling polycrystals with complex microstructures

R.A Lebensohn [a,*], P.A. Turner [a], G.R. Canova [b]

[a] *Instituto de Física Rosario (UNR-CONICET), 27 de Febrero 210 Bis, 2000 Rosario, Argentina*
[b] *GPM2, ENSPG Domaine Universitaire, BP 46, 38402 St. Martin d'Heres, France*

Abstract

This paper presents recent advances in modelling mechanical behavior of polycrystalline materials having some kind of spatial correlation between neighbour crystals. In the case of a lamellar $(\alpha+\beta)$ alloy, we use a 2-site viscoplastic selfconsistent (VPSC) model to show that the correlation between phases has a relevant influence on texture development. In the case of a TiAl intermetallic, we consider a stacking sequence of lamellar twins deforming as an ensemble. This leads to a local constitutive behavior different from the one expected for a single crystal and, therefore, gives a different plastic response at macroscopic level. © 1997 Elsevier Science B.V.

PACS: 62.20.fe; 81.40; 82.20.wt

Keywords: Two-phase polycrystals; Lamellar structures; Selfconsistent model

1. Introduction

In the present work we are concerned with the prediction of plastic behavior and texture development of heterogeneous materials with complex microstructures. We will focus our analysis on two-phase polycrystals and single-phase materials with a lamellar structure. Modelling plasticity of these kind of materials requires more sophisticated formulations than those provided by the classical Taylor full (FC) [1] and relaxed constraints (RC) [2] hypothesis. These classical polycrystalline models usually give acceptable results when applied to single-phase non-correlated materials, in which the major source of heterogeneity in the local plastic response is given by the difference in orientation of the constituent anisotropic crystallites. In a two-phase polycrystal, instead, the two phases may exhibit large differences in critical stresses, strain-rate sensitivity, microscopic work-hardening or grain shape. These differences can be accounted for by means of large strain selfconsistent approaches [3,4]. In fact, several authors [5–7] have used the 1-site viscoplastic selfconsistent (VPSC-1S) approach to model texture development of two-phase polycrystals, obtaining satisfactory results.

The VPSC-1S approach, however, is not enough to account for some important microstructural features of some kind of two-phase polycrystals. Several two-phase materials exhibit a strong crystallographic and morphologic correlation between phases

* Corresponding author. Tel.: +54-41-212028; fax: +54-41-821772; e-mail: ricardo@ifir.ifir.edu.ar.

PII S0927-0256(97)00078-5

that may give a non-negligible influence in the overall plastic response. This vicinity effect can obviously not be accounted for within the frame of a 1-site model. A general n-sites approach [3,8] should give a good representation of this kind of correlated polycrystals. However, whereas both phases usually form a stack and the correlation is periodically repeated, it turns out to be a good enough approximation to consider two interacting regions of different phases deforming embedded in an effective medium. Having this in mind, we present here two different approaches to consider interaction between correlated neighbour regions.

We present a micro–macro approach, an extension of the VPSC-1S called a *2-sites viscoplastic selfconsistent model* (VPSC-2S), and make use of it to discuss some aspects of texture formation in lamellar $(\alpha+\beta)$ Ti alloys. In these alloys, the regions corresponding to one phase are plane layers and each region of a given phase is always neighbour to a region of the other phase. Their crystallographic orientation is also subjected to certain rules described by the Burgers relation that puts one given crystallographic line and plane of one grain in coincidence with another plane and line of the other grain.

The second approach we present here, called a *lamellar structure model* (LS), is specially conceived to describe the local mechanical behavior of polysynthetically twinned (PST) crystals of γ-TiAl. Furthermore, we will also discuss how this LS model can be used as microscopic constitutive relation in the frame of any micro–macro approach to deal with an aggregate of families of correlated, very flat regions that form stacks or *lamellar structures*. For these materials it is more adequate to consider, at the microscopic level, the constitutive behavior of these lamellar structures, rather than the usual set of individual grains.

2. Models and results

2.1. VPSC-2S model: Texture development of lamellar $(\alpha+\beta)$ Ti alloys

In a 'correlated' two-phase polycrystal, like the lamellar $(\alpha+\beta)$ Ti alloys, the regions corresponding to both phases are layers and their relative crystallographic orientations are subjected to the Burgers relation. For modelling purposes, this microstructure can be represented as an aggregate of pairs of sites. The VPSC-2S model acts in solving the problem of each pair of sites considered as two viscoplastic inhomogeneities embedded in an effective medium which has the average properties of the polycrystal. The main equations of VPSC-2S together with a comparison with similar equations corresponding to the 1-site approach are summarized in Table 1. A thorough description of the model and the explicit expressions for Eshelby, interaction, localization and rotation tensors can be found in Ref. [9].

Depending on the previous thermomechanical treatments, the $(\alpha+\beta)$ Ti alloys exhibit two different kinds of microstructures, i.e. globular and lamellar. While in the former case the grains of both phases are approximately equiaxed and there is no correlation between the orientations of two neighbour α- and β-grains, in the latter very elongated α-grains grow inside initially large β-grains. The final structure consists of elongated α- and β-regions, correlated by the Burgers relation [10]. Two important correlations between α- and β-planes and directions are given by: $\{10\bar{1}0\}_\alpha//\{112\}_\beta$ $\langle 1\bar{2}10\rangle_\alpha//\langle 111\rangle_\beta$ and the habit plane between phases is the $\{5\bar{1}40\}_\alpha$, near to $\{10\bar{1}0\}_\alpha$ [10].

Fig. 1a shows the rolling texture (basal poles) after 70% thickness reduction of a lamellar alloy with 22% β-content [7]. The other five are theoretical rolling textures (same strain and 20% β-content) with the 1-site or 2-sites models, for different assumptions about the initial microscopic correlation between phases. In all cases, the active slip modes were assumed to be $\{1\bar{1}0\}\langle 111\rangle$ and $\{11\bar{2}\}\langle 111\rangle$ in the β-phase and $\{10\bar{1}0\}\langle 1\bar{2}10\rangle$, $(0001)\langle 1\bar{2}10\rangle$ and $\{10\bar{1}1\}\langle 1\bar{2}13\rangle$ in the α-phase. The first two slip modes ($\langle$a$\rangle$-slip) are assumed to be four times harder than the β-phase slip modes and the latter ($\langle$c + a$\rangle$ slip) eight times harder.

The five simulations were performed assuming an initial random texture of each phase. In the non-correlated cases (Fig. 1b and d), the $(\alpha+\beta)$ pairs were formed randomly. Also an arbitrary morphologic orientation was assigned to each pair. On the other hand, the initial configuration of the fully correlated

Table 1
Summary of the VPSC-2S equations and comparison with the 1-site approach

Equation	1S	2S
Inclusion[a]	$\tilde{\dot{\epsilon}} = S:\dot{\epsilon}^*$	$\tilde{\dot{\epsilon}}^1 = S^{11}:\dot{\epsilon}^{*1} + S^{12}:\dot{\epsilon}^{*2}$ $\tilde{\dot{\epsilon}}^2 = S^{21}:\dot{\epsilon}^{*1} + S^{22}:\dot{\epsilon}^{*2}$
Interaction[b]	$\tilde{\dot{\epsilon}} = -\tilde{M}:\tilde{\sigma}'$	$\tilde{\dot{\epsilon}}^1 = -\tilde{M}^{11}:\tilde{\sigma}'^1 - \tilde{M}^{12}:\tilde{\sigma}'^2$ $\tilde{\dot{\epsilon}}^2 = -\tilde{M}^{21}:\tilde{\sigma}'^1 - \tilde{M}^{22}:\tilde{\sigma}'^2$
Localization[c]	$\sigma' = B^c:\sigma'$	$\sigma'^1 = B^{c1}:\sigma'$ $\sigma'^2 = B^{c2}:\sigma'$
SC relation[d]	$M = \langle M^c:B^c \rangle$	$M = \langle M^{c1}:B^{c1} \rangle + \langle M^{c2}:B^{c2} \rangle$
Micro–macro	$\Sigma' = M^{-1}:\dot{E}$	$\Sigma' = M^{-1}:\dot{E}$
	$\dot{\epsilon}(\sigma') - \dot{E} = -\tilde{M}:(\sigma' - \Sigma')$	$\dot{\epsilon}^1(\sigma'^1) - \dot{E} = -\tilde{M}^{11}:(\sigma'^1 - \Sigma') - \tilde{M}^{12}:(\sigma'^2 - \Sigma')$ $\dot{\epsilon}^2(\sigma'^2) - \dot{E} = -\tilde{M}^{21}:(\sigma'^1 - \Sigma') - \tilde{M}^{22}:(\sigma'^2 - \Sigma')$
Rotations[e]	$\tilde{\omega} = \Pi:S^{-1}:\tilde{\epsilon}$	$\tilde{\omega}^1 = Y^{11}:\tilde{\epsilon}^1 + Y^{12}:\tilde{\epsilon}^2$ $\tilde{\omega}^2 = Y^{21}:\tilde{\epsilon}^1 + Y^{22}:\tilde{\epsilon}^2$

Notation: $\dot{E} - \Sigma'$: macro strain-rate and deviatoric stress. $\dot{\epsilon} - \sigma'$, $\dot{\epsilon} - \sigma'^1$, $\dot{\epsilon} - \sigma'^2$: micro strain-rates and deviatoric stresses. $\tilde{\dot{\epsilon}} - \tilde{\sigma}'$, $\tilde{\dot{\epsilon}}^1 - \tilde{\sigma}'^1$, $\tilde{\dot{\epsilon}}^2 - \tilde{\sigma}'^2$: local deviations in strain-rates and deviatoric stresses. $\tilde{\omega}$, $\tilde{\omega}^1$, $\tilde{\omega}^2$: local rotations rates.
[a] S, S^{11}, S^{22}: 1-site Eshelby tensors; S^{12}, S^{21}: 2-site Eshelby tensors.
[b] $\tilde{M}$, $\tilde{M}^{\alpha\beta}$ (α, $\beta = 1, 2$): interaction tensors.
[c] M^c, M^{c1}, M^{c2}: secant microscopic compliance; B^c, B^{c1}, B^{c2}: localization tensors.
[d] M: secant macroscopic compliance; $\langle\ \rangle$: weighted average.
[e] Π: skewsymmetric Eshelby tensor; Y^{IJ}: rotation tensors (functions of S^{IJ} and Π^{IJ}).

cases (Fig. 1c and f) consists in α-orientations related with β-orientations that fulfill the Burgers relation. Moreover, the morphologic orientation was selected so as to align the short axes of the ellipsoids (i.e. the habit plane's normal) with a $\{10\bar{1}0\}_\alpha$ plane. Finally, in the intermediate case of Fig. 1e, the reorientations are correlated with the α-ones but the morphologic orientation of each pair was randomly selected, so as to get a random orientation of the habit plane.

Although the simulations were carried out assuming an initial morphology of flat grains, both 1S textures (non-correlated and correlated cases) resemble the experimental textures measured in globular materials (i.e. a mild $\{hkil\}\langle 10\bar{1}0\rangle$ fiber [5–7]). Both results were expected. In the first case, the non-correlated configuration is obviously compatible with the globular material. In the latter case, the initial correlation does correspond to a lamellar case but the 1S model itself is unable to account for the vicinity effects which may affect the texture formation.

The VPSC-2S non-correlated texture is not very different from the 1S ones. Since the pairs were randomly selected, the overall neighbour effect is, therefore, canceled. Moreover, if only the crystallographic, but not the morphologic, correlation is considered, the predictions are not improved (Fig. 1e). This means that the orientation of the habit plane may also be relevant. In fact, only the 2S fully correlated simulation (Fig. 1f) shows the actual basal maximum in TD. In conclusion: the mean features of the texture of a lamellar material is well reproduced only if the actual correlations between phases are properly taken into account.

This better agreement between the actual α-texture and the 2S correlated predictions can be explained in terms of a higher activity of prismatic slip in the α-phase. An increment in the relative prismatic slip activity is indeed observed in the 2S full correlated case, compared with similar 1S results. In the case of lamellar ($\alpha + \beta$) Ti alloys, each pair of normal and Burgers vectors of the $\{10\bar{1}0\}\langle 1\bar{2}10\rangle$ prismatic slip mode in the α-phase is parallel to another pair of normal and Burgers vectors of the $\{11\bar{2}\}\langle 111\rangle$ slip mode in the β-phase and these $\{10\bar{1}0\}_\alpha$ and $\{11\bar{2}\}_\beta$ planes are, in turn, almost paral-

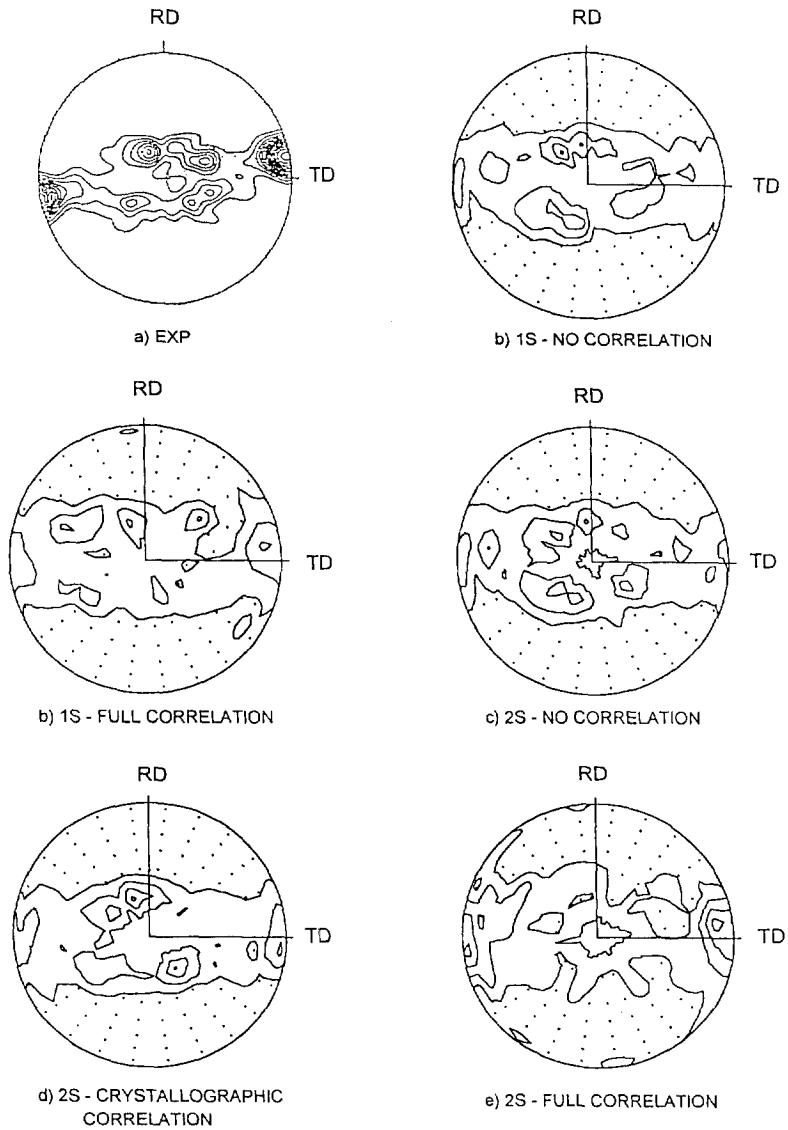

Fig. 1. (a) Measured α-textures (basal pole figure) of a lamellar ($\alpha + \beta$) Ti-alloy with 22% β-content, hot-rolled up to 70% thickness reduction [7]. (b–e) VPSC 1-site and 2-site calculated α-textures, 20% β-content, rolled up to 70% thickness reduction, assuming different morphologic and crystallographic correlations between phases. Lines are the multiple of random distribution (mrd). Dots are orientations below 1 mrd.

lel to the habit plane. Therefore, following Ankem and Margolin [10], the simultaneous activation in each phase of these 'parallel' slip systems should be favoured since it makes easier the slip transfer across the interface. This expected increment of prismatic slip activity in the fully correlated case leads to an enhancement of the transverse component in the α-texture since the prismatic slip in hexagonals is known to give rolling textures with a strong basal TD component [11].

2.2. LS model: Plastic behavior of γ-TiAl PST crystals

The aim of the LS model is to determine the plastic response of a PST crystal (for a detailed description of these structures see, for example, Ref. [12]). According to Mecking et al. [13], the active deformation modes of a γ-TiAl single crystal are: $\{111\}\langle 110]$ slip by ordinary dislocations, $\{111\}\langle 011]$ slip by super dislocations and $\{111\}\langle 11\bar{2}]$ twinning. In the present formulation, twinning is treated as an additional deformation mode with an assigned critical resolved shear stress. Unlike slip, the twinning is not operative in the opposite sense of the twinning vector.

The simplest structure that can be considered is that formed by a matrix and a twin. If, for instance, they correspond to a $(\bar{1}\bar{1}1)[\bar{1}\bar{1}2]$ twin, the reference frame that should be adopted is the one having axis x_1 lying along the twinning direction $[\bar{1}\bar{1}2]$, axis x_3 normal to the twinning plane and axis x_2 along the $[1\bar{1}0]$ direction.

When a given strain-rate $\dot{\epsilon}$ is applied to a single crystal, its plastic response can be described by means of the rate-sensitive approach:

$$\dot{\epsilon}_i = \dot{\gamma}_0 \sum_s m_i^s \left(\frac{m_j^s \sigma_j'}{\tau^s} \right)^n \tag{1}$$

where σ' is the deviatoric stress tensor in the single crystal, m^s and τ^s are the Schmid tensor and the critical stress for system s, $\dot{\gamma}_0$ is a reference strain-rate and n is the inverse of the rate sensitivity. In Eq. (1), the traceless tensors are expressed as vectors using a modified Lequeu [14] convention [1]. From Eq. (1), a 5×5 non-linear system should be solved to obtain the 5 components of σ_j'.

[1] Modified Lequeu convention: $T_1 = 1/\sqrt{2}(T_{22} - T_{11})$; $T_2 = \sqrt{3/2}\,T_{33}$; $T_3 = \sqrt{2}\,T_{12}$; $T_4 = \sqrt{2}\,T_{13}$ and $T_5 = \sqrt{2}\,T_{23}$, where T_k is the vectorial representation of tensor T_{ij}.

On the other hand, considering a PST crystal made of 2 lamellae, I and II, of the same volume, the constitutive relation can be written as:

$$\bar{\dot{\epsilon}}_i = \dot{\gamma}_0 \left(\frac{1}{2} \sum_s m_i^{s,\mathrm{I}} \left(\frac{m_j^{s,\mathrm{I}} \sigma_j'^{\mathrm{I}}}{\tau^{s,\mathrm{I}}} \right)^n + \frac{1}{2} \sum_s m_i^{s,\mathrm{II}} \left(\frac{m_j^{s,\mathrm{II}} \sigma'^{\mathrm{I}}{}_j}{\tau^{s,\mathrm{II}}} \right)^n \right) \tag{2a}$$

$$\dot{\epsilon}_1^{\mathrm{I}} = \dot{\epsilon}_1^{\mathrm{II}} \tag{2b}$$

$$\dot{\epsilon}_2^{\mathrm{I}} = \dot{\epsilon}_2^{\mathrm{II}} \tag{2c}$$

$$\dot{\epsilon}_3^{\mathrm{I}} = \dot{\epsilon}_3^{\mathrm{II}} \tag{2d}$$

$$\sigma_4'^{\mathrm{I}} = \sigma_4'^{\mathrm{II}} \ (= \sigma_4') \tag{2e}$$

$$\sigma_5'^{\mathrm{I}} = \sigma_5'^{\mathrm{II}} \ (= \sigma_5') \tag{2f}$$

where $\bar{\dot{\epsilon}}$ is the strain-rate applied to the PST, $(\dot{\epsilon}^{\mathrm{I}}; \sigma'^{\mathrm{I}})$ and $(\dot{\epsilon}^{\mathrm{II}}; \sigma'^{\mathrm{II}})$ are the local states inside lamellae I and II and s,I and s,II identify the deformation systems of lamellae I and II, respectively. We have assumed in writing Eq. (2a) that the overall strain-rate is given by a weighted average of the strain-rate inside each lamella. To illustrate this, we could think on an extreme case in which one lamella is not deforming at all. Then, this averaging assumption for the strain-rate would determine that the other lamella should undergo a local strain-rate equal to twice the applied one. Moreover, in writing Eqs. (2b), (2c), (2d), (2e) and (2f) we have used the usual relaxed constraints concept [2]: provided the lamellae are flat (being the short direction along x_3) the only differences in the local strain-rate components which can be accommodated without large spatial incompatibilities correspond to shears $\dot{\epsilon}_4$ $(\dot{\epsilon}_{23})$ and $\dot{\epsilon}_5$ $(\dot{\epsilon}_{13})$. Therefore, the continuity across the interface of the other three strain-rate components and of the 4th and 5th components of the stress should be enforced. Moreover, Eqs. (2e) and (2f) are two (out of three) necessary conditions for equilibrium of forces across the interface. The third condition, i.e. the continuity of the Cauchy stress component across the interface $(\sigma_{33}^{\mathrm{I}} = \sigma_{33}^{\mathrm{II}})$, can be also fulfilled by imposing adequate hydrostatic states inside each lamella.

With Eqs. (2a), (2b), (2c) and (2d), and using conditions Eqs. (2e) and (2f), it is possible to build an 8×8 non-linear system of equations where the

unknowns are $\sigma_1'^{\mathrm{I}}$, σ_2^{I}, $\sigma_3'^{\mathrm{I}}$; $\sigma_1'^{\mathrm{II}}$, $\sigma_2'^{\mathrm{II}}$, $\sigma_3'^{\mathrm{II}}$ and σ_4', σ_5'. Eqs. (2a), (2b), (2c), (2d), (2e) and (2f) can be extended to the case of a structure with N lamellae, each of them having different orientation and volumes:

$$\bar{\dot{\epsilon}} = \dot{\gamma}_0 \sum_{K=1}^{N} w^K \sum_s m_i^{s,K} \left(\frac{m_j^{s,K} \sigma_j'^K}{\tau^{s,I}} \right)^n \tag{3a}$$

$$\dot{\epsilon}_1^{\mathrm{I}} = \dot{\epsilon}_1^{\mathrm{II}} = \ldots = \dot{\epsilon}_1^N \tag{3b}$$

$$\dot{\epsilon}_2^{\mathrm{I}} = \dot{\epsilon}_2^{\mathrm{II}} = \ldots = \dot{\epsilon}_2^N \tag{3c}$$

$$\dot{\epsilon}_3^{\mathrm{I}} = \dot{\epsilon}_3^{\mathrm{II}} = \ldots = \dot{\epsilon}_3^N \tag{3d}$$

$$\sigma_4'^{\mathrm{I}} = \sigma_4'^{\mathrm{II}} = \ldots = \sigma_5'^N \tag{3e}$$

$$\sigma_5'^{\mathrm{I}} = \sigma_5'^{\mathrm{II}} = \ldots = \sigma_5'^N \tag{3f}$$

where w^K is the volume fraction of lamella K with respect to the whole structure. In the TiAl case, provided the four twinning systems have different twinning planes (see Table 1), the most general lamellar structure is a stacking sequence of matrix (M) and twinned (T) regions (i.e.: M–T–M–T–...). Hence, if w^{M} and w^{T} are the volume fractions of the matrix and the twinned regions, respectively, Eqs. (2a), (2b), (2c), (2d), (2e) and (2f) can be rewritten as:

$$\bar{\dot{\epsilon}} = \dot{\gamma}_0 \left(w^{\mathrm{M}} \sum_s m_i^{s,\mathrm{M}} \left(\frac{m_j^{s,\mathrm{M}} \sigma_j'^{\mathrm{M}}}{\tau^{s,\mathrm{M}}} \right)^n + w^{\mathrm{T}} \sum_s m_i^{s,\mathrm{T}} \left(\frac{m_j^{s,\mathrm{T}} \sigma_j'^{\mathrm{T}}}{\tau^{s,\mathrm{T}}} \right)^n \right) \tag{4a}$$

$$\dot{\epsilon}_1^{\mathrm{M}} = \dot{\epsilon}_1^{\mathrm{T}} \tag{4b}$$

$$\dot{\epsilon}_2^{\mathrm{M}} = \dot{\epsilon}_2^{\mathrm{T}} \tag{4c}$$

$$\dot{\epsilon}_3^{\mathrm{M}} = \dot{\epsilon}_3^{\mathrm{T}} \tag{4d}$$

$$\sigma_4'^{\mathrm{M}} = \sigma_4'^{\mathrm{T}} \tag{4e}$$

$$\sigma_5'^{\mathrm{M}} = \sigma_5'^{\mathrm{T}} \tag{4f}$$

Eqs. (1), (4a), (4b), (4c), (4d), (4e) and (4f) can be solved to get π-plane projections of the yield surface (YS) of each single crystal (i.e. each individual lamella) and lamellar structure, respectively. The $\{\pi\}$-projection is the locus of points for which $\dot{\epsilon}_3 = \dot{\epsilon}_4 = \dot{\epsilon}_5 = 0$ [15]. Therefore, the single crystal or lamellar structure must be proven in different directions in the deviatoric plane to obtain the stress σ' in the single crystal or the local stresses σ'^{I}, σ'^{II} in the lamellae. In the latter case, the overall stress is given by:

$$\bar{\sigma}_i = w^{\mathrm{M}} \sigma_i'^{\mathrm{M}} + w^{\mathrm{T}} \sigma_i'^{\mathrm{T}} \tag{5}$$

The stress vector $\bar{\sigma}$ gives a point of the YS for which the normal to the YS lies along the $\bar{\dot{\epsilon}}$ direction. With a point and the normal it is possible to trace a tangent plane to the YS. The inner envelope of the set of tangent planes gives a good approximation to the actual YS. The magnitudes of the various $\bar{\dot{\epsilon}}$ are so that all the states correspond to the same plastic potential.

Fig. 2 displays the single crystal yield surface (SCYS) of the matrix and the twin, considered as single crystals and the yield surfaces of two lamellar structures (LYS), corresponding to a $w^{\mathrm{M}} = w^{\mathrm{T}} = 0.5$ (50–50 case) and $w^{\mathrm{M}} = 0.75$, $w^{\mathrm{T}} = 0.25$ (75–25 case). In both cases, the critical stresses of ordinary slip, super slip and twinning are assumed to be equal to 1, in arbitrary units. Due to symmetry, both SCYS projections are coincident. In the 50–50 case, the lamellar structure is softer than the individual single crystals, specially for loading paths which are close to uniaxial stress states along x_2. Also, by comparing the results for various volume fractions, it is

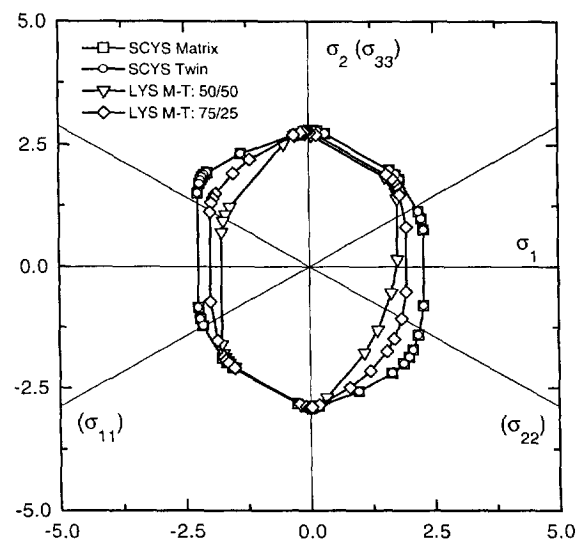

Fig. 2. Yield surfaces of two single crystals (SCYS) having the matrix orientation and the $(\bar{1}11)[\bar{1}\bar{1}2]$ twin orientation and of two lamellar structures (LYS) formed by those matrix and twin crystals, in 50–50 and 75–25 proportions. The reference frame is $x_1 \equiv [\bar{1}\bar{1}2]$, $x_2 \equiv [1\bar{1}0]$ and $x_3 \equiv [\bar{1}\bar{1}1]$.

clear that the 75–25 is located in between the 50–50 and the SCYS cases. It follows that, if some mechanical twins are formed inside a grain and they tend to grow as deformation proceeds, the 'softening' effect will smoothly increase, together with the increasing of the twinned volume fraction. The predicted anisotropy of the PST crystals are in good agreement with most of the available experimental data [12]. A comparison between model predictions and experiments can be found elsewhere [16]. This simple model for the description of the plastic behavior of lamellar structures can be used as local constitutive equation of any polycrystalline approach. It can be implemented, for example, inside a FC Taylor model. In this case, for every lamellar structure in an aggregate, $\bar{\dot{\epsilon}}_i$ in Eq. (4) is given by the following micro–macro connection:

$$\bar{\dot{\epsilon}}_i = \dot{E}_i^{ap} \tag{6}$$

where $\dot{E}_i^{ap}$ is the strain-rate applied to the polycrystal. It is also possible to use the LS model as local constitutive behavior in a VPSC 1-site model. For this it is necessary to know the expression of the local tangent modulus of the structure.

$$\bar{M}_{ij}^{tg} = \frac{d\bar{\dot{\epsilon}}_i}{d\bar{\sigma}_j} \tag{7}$$

The expression of $\bar{M}_{ij}^{tg}$ for a matrix–twin structure (with volume fractions w^M and w^T, respectively) is given by:

$$\bar{M}^{tg} = \left[w^M M^{tg,M} : A + w^T M^{tg,T}\right] : \left[w^M A + w^T I\right]^{-1} \tag{8}$$

where $M^{tg,M}$ and $M^{tg,T}$ are the tangent moduli of each single crystal and:

$$A = \left[K : \tfrac{1}{n} M^{tg,M} + I\right]^{-1} : \left[K : \tfrac{1}{n} M^{tg,T} + I\right] \tag{9}$$

with:

$$K = \begin{bmatrix} \infty & 0 & 0 & 0 & 0 \\ 0 & \infty & 0 & 0 & 0 \\ 0 & 0 & \infty & 0 & 0 \\ 0 & 0 & 0 & 0 & 0 \\ 0 & 0 & 0 & 0 & 0 \end{bmatrix}$$

$$\simeq \begin{bmatrix} 10^m & 0 & 0 & 0 & 0 \\ 0 & 10^m & 0 & 0 & 0 \\ 0 & 0 & 10^m & 0 & 0 \\ 0 & 0 & 0 & 10^{-m} & 0 \\ 0 & 0 & 0 & 0 & 10^{-m} \end{bmatrix} \tag{10}$$

where the latter matrix is a handy approximation of the former one, with $m \gg 1$.

The derivation of these expressions together with the numerical implementation of these coupling between the local LS model an the VPSC-1S formulation can be found elsewhere [17]. It is worth noting that this approach 'in two scales' should give essentially the same results as the VPSC-2S approach in its limit for extremely flat grains.

3. Conclusions

Concerning the VPSC-2S model and the $(\alpha + \beta)$ Ti alloys:

(1) We showed that, only with a model which is able to account for the local spatial correlations, is it possible to predict the main features of the texture development in highly correlated two-phase materials.

(2) In the case of rolled lamellar $(\alpha + \beta)$ Ti alloys with low β-content, the TD component in the α-phase is related to the preferred activity of prismatic slip associated with the Burgers crystallographic relation and the particular orientation of the habit plane.

Concerning the LS model and the TiAl PST material:

(1) We proposed some simple equations to find the plastic behavior of a lamellar structure. The correlation between the local states inside each lamella are based on the relaxed constraint concepts.

(2) In the TiAl case, the particular symmetry of matrix–twin pair allows a cooperative mechanism of deformation of the lamellae which, for certain loading paths, makes the structure to be softer than the single crystals alone.

(3) We showed how the LS model can be coupled with a polycrystal formulation, both in a simple FC case or in a more sophisticated selfconsistent case.

References

[1] G.I. Taylor, J. Inst. Metals 62 (1938) 307.
[2] H. Honneff, H. Mecking, in: S. Nagashima (Ed.), Proc. Sixth Int. Conf. on Texture of Materials, ICOTOM-6, Iron and Steel Inst. Japan, Tokyo, 1981, p. 347.

[3] A. Molinari, G.R. Canova, S. Ahzi, Acta Metall. 35 (1987) 2983.
[4] R.A. Lebensohn, C.N. Tomé, Acta Metall. Mater. 41 (1993) 2611.
[5] B. Bacroix, G.R. Canova, H. Mecking, in: C. Teodosiu, J.L. Raphanel (Eds.), Proc. MECAMAT'91, Balkema, Rotterdam, 1993, p. 101.
[6] D. Dunst, R. Dendievel, H. Mecking, Mater. Sci. Forum 157-162 (1994) 665.
[7] D. Dunst, H. Mecking, Z. Metallkd. 87 (1996) 506.
[8] G.R. Canova, H.R. Wenk, A. Molinari, Acta Metall. Mater. 40 (1992) 1519.
[9] R.A. Lebensohn, G.R. Canova, Acta Mater. (1997), in press.
[10] S. Ankem, H. Margolin, Met. Trans. A 17A (1986) 2209.
[11] R.A. Lebensohn, Ph.D. Thesis, Universidad Nacional de Rosario, Argentina, 1993.
[12] M. Yamagushi, ISIJ Int. 31 (1991) 1127.
[13] H. Mecking, C. Hartig, U.F. Kocks, Acta Mater. 44 (1996) 1309.
[14] P. Lequeu, P. Gilormini, F. Montheillet, B. Bacroix, J.J. Jonas, Acta Metall. 35 (1987) 439.
[15] G.R. Canova, U.F. Kocks, C.N. Tomé, J.J. Jonas, J. Mech. Phys. Solids 33 (1985) 371.
[16] H. Uhlenhut, R.A. Lebensohn, C. Hartig, H. Mecking, this conference.
[17] R.A. Lebensohn, G.R. Canova, to be published.